Hindawi
Journal of Chemistry
Volume 2023, Article ID 8897036, 9 pages
https://doi.org/10.1155/2023/8897036

Research Article

A Simple Ratiometric Electrochemical Aptasensor Based on Exonuclease III-Assisted Target Recycling for Ultrasensitive Detection of Prostate Specific Antigen

Ping Wang, Yaoyao Xie, Zhimin Guan, Huikai Ma, and Shoumin Xi

College of Basic Medicine and Forensic Medicine, Henan University of Science and Technology, Luoyang 471000, China

Correspondence should be addressed to Ping Wang; glorywangping@163.com and Shoumin Xi; xishoumin1968@163.com

Received 8 May 2023; Revised 3 August 2023; Accepted 4 August 2023; Published 11 August 2023

Academic Editor: Takeshi Kondo

Prostate specific antigen (PSA) is considered as an important biomarker in prostate cancer diagnosis. Herein, an ultrasensitive ratiometric electrochemical aptasensor was constructed for analyzing PSA. The ferrocene (Fc)-labeled thiolated hairpin probe 2 (Fc-HP2) was conjugated to the gold nanoparticles (AuNPs)-modified gold electrode (AuE) surface by Au-S bonds. With the introduction of PSA, the aptamer region of hairpin probe 1 (HP1) preferred to bind with PSA, and the rest of HP1 could hybridize with Fc-HP2 to form Fc-HP2/HP1/PSA complex with a blunt 3′ terminus, which triggered the exonuclease III (Exo III) cleavage process accompanied by Fc leaving from the electrode and recycling of HP1/PSA. The remaining Fc-HP2 fragments left on the electrode surface were then hybridized with methylene blue-labeled DNA (MB-DNA). This resulted in an enhancement of MB signal (I_{MB}) and a decrement of Fc signal (I_{Fc}). Under the optimal conditions, the proposed aptasensor showed good analytical performance for sensitive detection of PSA with a linear range from 100 fg·mL^{-1} to 10 ng·mL^{-1} and a detection limit of 34.7 fg·mL^{-1}. The fabricated aptasensor had been applied to detect PSA in diluted human serum samples and obtained satisfied results, suggesting it had great potential in clinical diagnosis.

1. Introduction

Prostate cancer is one of the most common types of cancer affecting men worldwide, and in early stages, the symptoms are not obvious. When found in late stages, the mortality rate is high [1, 2]. Therefore, detection in its early stage is critical for the successful treatment of prostate cancer and it improves the survival rates. Prostate specific antigen (PSA), a single-chain serine protease produced by the epithelial cells of the prostate gland, is a commonly used biomarker in prostate cancer diagnosis [3]. In healthy male serum, the concentration of PSA is lower than 4.0 ng·mL^{-1}, and serum PSA levels above 10 ng·mL^{-1} are likely to develop prostate cancer [1, 4]. Therefore, establishment of an ultrasensitive and simple method for the analysis of low levels of PSA is of great significance for the early diagnosis of prostate cancer.

Currently, a series of detection methods have been used for the detection of PSA, such as enzyme-linked immunosorbent assay (ELISA) [5], surface-enhanced Raman scattering (SERS) [6], colorimetric method [7], chemiluminescence immunoassay [8], and electrochemical methods [9, 10]. Among them, electrochemical methods have attracted the attention of researchers due to their high sensitivity, simple operation, low cost, and potential for miniaturization.

Early PSA electrochemical biosensors usually used antibody-based approaches, and other recognition elements, such as aptamers, are gaining the attention today. Aptamers are single-stranded DNA or RNA oligonucleotides isolated using systematic evolution of ligands by exponential enrichment (SELEX) [11]. They are capable of binding to a number of targets including proteins, small molecules, metal ions, viruses, bacteria, and even the whole cell with high affinity and specificity [12–14]. Compared with

conventional antibodies, aptamers possess unique advantages such as high selectivity, low cost, better stability, and ease of chemical modification [15]. Different aptasensing platforms for PSA detection have been recently developed [16–19].

To improve the detection sensitivity, various signal amplification strategies are used to amplify the electrochemical signals. Among them, enzyme digestion amplification method [20] has been widely used recently. For example, exonuclease III (Exo III)-assisted target recycling amplification has emerged as a powerful amplification technique and attracted great attention due to its ease of operations and the simplicity of equipment [21–25]. Besides detection sensitivity, the reproducibility, stability, and reliability are also important indicators to investigate the performance of the sensors. Most of the reported electrochemical sensors used a single signal output, which are easily affected by internal or external factors such as electrode and environment. However, the ratiometric strategy [26–28] which uses two independent electrochemical signals of probes has been introduced to overcome the limitations. Methylene blue (MB) and ferrocene (Fc) are mainly selected as electrochemical species to fabricate ratiometric electrochemical aptasensors [29–32]. The analyte concentration can be determined by using the ratio of the peak current intensity of two electroactive probes. Therefore, the accuracy and reproducibility of detection can be greatly improved by eliminating the interference of the possible external and internal influence [33].

Herein, a simple ratiometric electrochemical aptasensor based on Exo III-assisted target recycling amplification was constructed for the detection of PSA (Scheme 1). Firstly, the gold nanoparticles (AuNPs)-modified gold electrode (AuE) was obtained through in situ electro deposition (AuNPs/AuE electrode). Subsequently, Fc-labeled hairpin probe 2 (Fc-HP2) was self-assembled onto the AuNPs/AuE surface via Au-S bond, and Fc was close to the electrode surface. MCH was used to the block the unbound sites. In the presence of target PSA, the aptamer sequence (red region) of hairpin probe 1 (HP1) bound specifically with PSA, and the hairpin structure of HP1 was opened to form HP1/PSA complex. Then, the rest fragment of HP1 (black region) hybridized with Fc-HP2 to form Fc-HP2/HP1/PSA complex with a blunt 3′ terminus. In the presence of Exo III, it could recognize the Fc-HP2/HP1/PSA complex and catalyze stepwise removal of mononucleotides from the blunt 3′ terminus, which led to the releasing of Fc molecules and liberating HP1/PSA complex to achieve Exo III-assisted signal amplification. The Fc-HP2 fragments left on the sensor surface were then hybridized with MB-labeled DNA (MB-DNA), making the MB confined near the electrode. As a result, the ratiometric assay for PSA detection based on the decrease of oxidation peak current of Fc (I_{Fc}) and accompanied by the increase of that of I_{MB} was achieved. By measuring the ratio of I_{MB}/I_{Fc}, PSA could be quantitatively analyzed. By combining the Exo III-assisted target recycling and ratiometric dual-signal strategy, the aptasensor has the advantage of good specificity and reproducibility and high sensitivity and low detection limit.

2. Experimental Section

2.1. Reagents and Materials. Hydrogen tetrachloroaurate trihydrate ($HAuCl_4 \cdot 3H_2O$, ≥99.9%), tris (2-carboxyethyl) phosphine (TCEP, 98%), and 6-mercapto-1-hexanol (MCH, 98%) were all acquired from Shanghai Aladdin Biochemical Technology Co., Ltd. (Shanghai, China). Exo III (100 $U \cdot \mu L^{-1}$) was obtained from New England Biolabs Ltd. (Beijing, China). PSA, carcinoembryonic antigen (CEA), alpha-fetoprotein (AFP) antigen, and human serum albumin (HSA) were purchased from Shanghai LincBio Science Co., Ltd. (Shanghai, China). Ultrapure water (18.2 MΩ·cm) was used for preparing the solutions. Tris-ethylenediaminetetraacetic acid (EDTA) (TE) buffer (10 mM Tris-HCl, 1 mM EDTA, and pH 8.0) was purchased from Sangon Biotechnology Co., Ltd. (Shanghai, China) and used to dilute DNA oligonucleotides. DNA immobilization buffer (I-buffer) was 20 mM Tris-HCl (50 mM NaCl, 10 mM $MgCl_2$, 10 mM TCEP, and pH 8.0); the electrode washing buffer (W-buffer) was 10 mM Tris-HCl (100 mM NaCl and pH 7.4); DNA hybridization buffer (H-buffer) was 10 mM Tris-HCl (1 mM EDTA, 500 mM NaCl, 1 mM $MgCl_2$, and pH 7.4). The solution for cyclic voltammetry (CV) and electrochemical impedance spectroscopy (EIS) was 0.1 M KCl solution containing 5 mM $[Fe(CN)_6]^{3-/4-}$ (1 : 1). The oligonucleotides used in the experiment were purchased from Sangon Biotechnology Co., Ltd. (Shanghai, China), and the sequences were as follows: hairpin probe 1 (HP1): 5′-TTT TTA ATT AAA GCT CGC CAT CAA ATA GCT TTG GCG AGC TTT AAC GTC GAC AC-3′; Fc-labeled hairpin probe 2 (Fc-HP2): 5′-SH-SH-$(CH_2)_6$-CCA TAG CTT TAA GTG CGA CGT TAA AGC TCG CC-Fc-3′; and MB-DNA: 5′-TTA AAG CTA TGG-MB-3′.

2.2. Apparatus and Measurements. The Autolab PGSTAT 128N station (Metrohm Autolab, The Netherlands) was used for CV and EIS tests, and other electrochemical measurements were performed on a CHI840D electrochemical workstation (CH Instrument, China). A traditional three-electrode system was used with a modified gold electrode (AuE, 2 mm) as the working electrode, a platinum wire as the counter electrode, and an Ag/AgCl electrode as reference electrode, respectively.

2.3. Fabrication of the Aptasensor and PSA Detection. The gold electrode (AuE) was polished following the reported method [34]. Then, gold nanoparticles (AuNPs) were electrodeposited on AuE in 10 mM $HAuCl_4$ solution at −0.2 V for 200 s to obtain AuNPs/AuE. Prior to attachment to the AuNPs/AuE surface, thiolated Fc-HP2 probe was mixed with TCEP (1 mM) for 1 h at room temperature and diluted to 1 μM with I-buffer for use. 5 μL of Fc-HP2 was applied to the AuNPs/AuE surface and incubated for 12 h at 4°C. After thoroughly rinsed with W-buffer, MCH (1 mM) was used to block the unoccupied binding sites for 1 h to obtain the sensing interface (MCH/Fc-HP2/AuNPs/AuE).

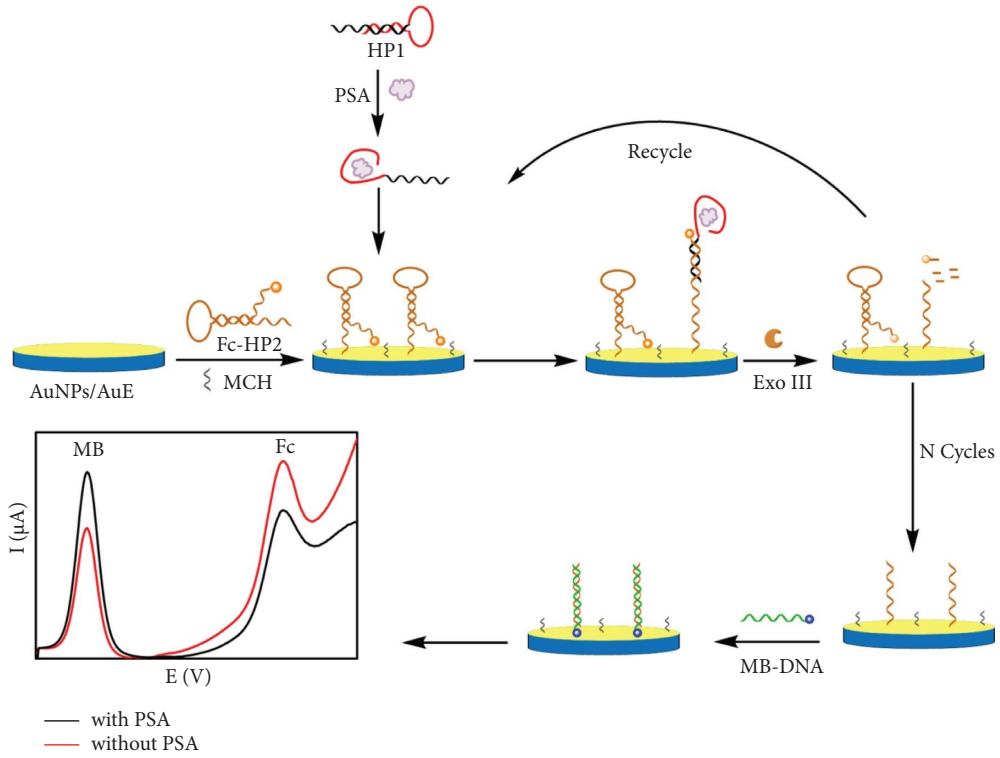

Scheme 1: Schematic illustration of the ratiometric electrochemical aptasensor for PSA detection.

Firstly, different concentrations of PSA were mixed with HP1 (1 μM) and Exo III (2 U) in 50 mM Tris-HCl (10 mM $MgCl_2$ and pH 7.4). Then, 5 μL of the above solution was dropped on the MCH/Fc-HP2/AuNPs/AuE surface and incubated for 80 min at 37°C to perform the Exo III-assisted recycling process. After washing with W-buffer, the modified electrode was incubated with MB-DNA (1 μM) in H-buffer at 37°C for 1 h and rinsed with ultrapure water. Finally, the electrode was subjected to the square-wave voltammetry (SWV) (step potential, 4 mV; frequency, 25 Hz; amplitude, 25 mV) test in 10 mM Tris-HCl (pH 7.4) from −0.4 to 0.6 V.

3. Results and Discussion

3.1. Feasibility of the Aptasensor. To illustrate the feasibility of the constructed aptasensor for PSA detection, a set of SWV experiments were conducted. As depicted in Figure 1, a low peak current of MB at −0.240 V and a high peak current of Fc at 0.368 V were observed when in the absence of PSA and Exo III (curve a). In the presence of only PSA (curve b) or Exo III (curve c), the SWV intensity almost changed compared to that of curve a, indicating that the PSA or Exo III alone could not trigger the amplification reaction. However, an obvious reduced Fc signal and increased MB signal were obtained in the presence of both PSA and Exo III (curve d), suggesting the occurrence of the Exo III-assisted signal amplification process and Fc was released from the electrode surface. Then, MB-DNA hybridized with the Fc-HP2 fragment was left on the electrode, and MB was near to the electrode surface. These results clearly demonstrated the feasibility of the ratiometric aptasensor for PSA detection.

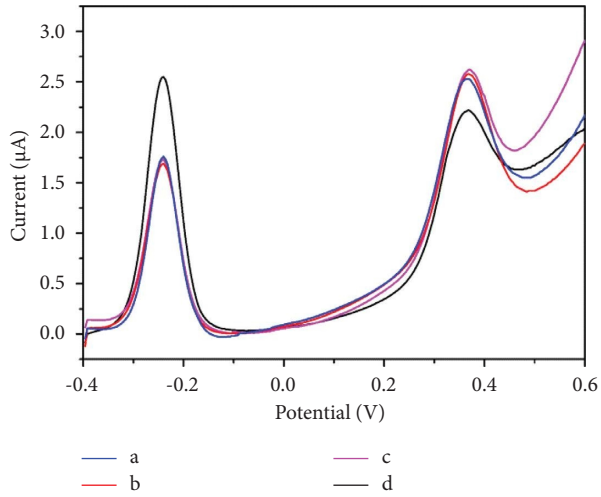

Figure 1: The feasibility of the strategy. (a) No PSA and no Exo III, (b) only PSA present, (c) only Exo III present, and (d) with PSA and Exo III.

3.2. Verification of Exo III-Assisted Target Recycling Process. 15% polyacrylamide gel electrophoresis (PAGE) was employed to verify the Exo III-assisted target recycling process. As shown in Figure 2, lane 1 and 2 represented the bands of HP1 and Fc-HP2, respectively. A new band with slower migration shift was observed (lane 3) after the hybridization of HP1 and Fc-HP2 with the presence of PSA. When Exo III was added, a new band

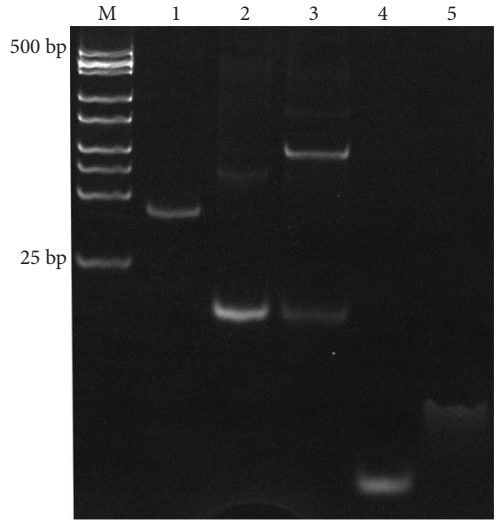

Figure 2: PAGE analysis of the Exo III-assisted target recycling process. Lane M: DNA marker, lane 1: HP1, lane 2: Fc-HP2, lane 3: HP1 + Fc-HP2 + PSA, lane 4: HP1 + Fc-HP2 + PSA + Exo III, and lane 5: HP1 + Fc-HP2 + PSA + Exo III + MB-DNA.

with faster migration shift was displayed in lane 4, which was attributed to the generation of short output DNAs digested from the duplex by Exo III. After the addition of MB-DNA, a band migrated slower than lane 4 was appeared due to the success of DNA hybridization (lane 5).

3.3. Characterization of the Modified Electrodes. The stepwise fabrication of the aptasensor was monitored by EIS and CV, and the results are displayed in Figures 3(a) and 3(b), respectively. Compared with the bare AuE (Figures 3(a) and 3(b), curve (a)), the value of electron transfer resistance (R_{et}) was significantly reduced and the corresponding redox peak current was obviously increased after being modified with AuNPs (Figures 3(a) and 3(b), curve (b)), implying the excellent electrical conductivity of AuNPs. The assembly of Fc-HP2 on the electrode surface led to an increase in R_{et} and a decrease of the redox peak current (Figures 3(a) and 3(b), curve (c)) due to the electrostatic repulsion between the negatively charged probes and $[Fe(CN)_6]^{3-/4-}$. Blocking with MCH led to a further enhancement in R_{et} and reduced redox peak current (Figures 3(a) and 3(b), curve (d)). Subsequently, HP1 recognized PSA and paired Fc-HP2 on the electrode to form a Fc-HP2/HP1/PSA complex. With the addition of Exo III, the R_{et} decreased obviously and the redox peak current increased (Figures 3(a) and 3(b), curve (e)), which was ascribed to the fact that Fc-HP2 probes were digested by Exo III. The introduction of MB-DNA on the electrode surface led to the increase of R_{et} and decrease of the redox peak current again (Figures 3(a) and 3(b), curve (f)), indicating the success of DNA hybridization. The CV results were in line with the EIS results, demonstrating the successful fabrication of the aptasensor.

3.4. Optimization of Experimental Conditions. The experimental conditions including the Fc-HP2 probe concentration, Exo III dosage, and incubation time of the Exo III were optimized, and the results are presented in Figure 4. As shown in Figure 4(a), the I_{MB}/I_{Fc} values increased when the concentration of Fc-HP2 increased from 0.25 to 1 μM and then began to decrease with the increasing of concentration, which may be due to the steric hindrance at high concentrations. Hence, 1 μM was the optimized concentration for Fc-HP2. The dosage of Exo III was also optimized. As displayed in Figure 4(b), increment in the concentration of Exo III from 0.5 to 2 U led to the increased in I_{MB}/I_{Fc} values and reached the maximum at 2 U. Therefore, 2 U was selected as the optimal dosage for Exo III. The effect of incubation time of Exo III was also investigated. In the range from 20 to 80 min, the I_{MB}/I_{Fc} values increased with the increase of time and reached the maximum at 80 min, indicating that the Fc-HP2 probes on the electrode surface were almost completely digested. Thus, the best incubation time of Exo III was 80 min (Figure 4(c)).

3.5. Analytical Performance of the Ratiometric Electrochemical Aptasensor. Under optimal experimental conditions, the proposed aptasensor was employed to detect PSA at different concentrations. Figure 5(a) demonstrates the relationship between the SWV responses and PSA concentration. With the increment of PSA concentration, more HP2 probes were digested by Exo III and many MB-DNA probes were captured on the electrode surface, so that I_{Fc} gradually decreased, while I_{MB} increased. Figure 5(b) showes the relationship between the peak currents and the logarithm of PSA concentration, and from the figure, we could see that the peak current of MB was positively related to logarithm of PSA concentration, while the peak current of Fc was negatively related to logarithm of PSA concentration. A good linear relationship between I_{MB}/I_{Fc} and the logarithm of PSA concentration in the range of 100 fg·mL^{-1} to 10 ng·mL^{-1} could be seen in Figure 5(c). The obtained linear equation was $I_{MB}/I_{Fc} = 0.102\ \lg C + 1.160$ ($R^2 = 0.9979$) with a limit of detection (LOD) of 34.7 fg·mL^{-1} ($S/N = 3$). In addition, our proposed aptasensor was compared with the previously

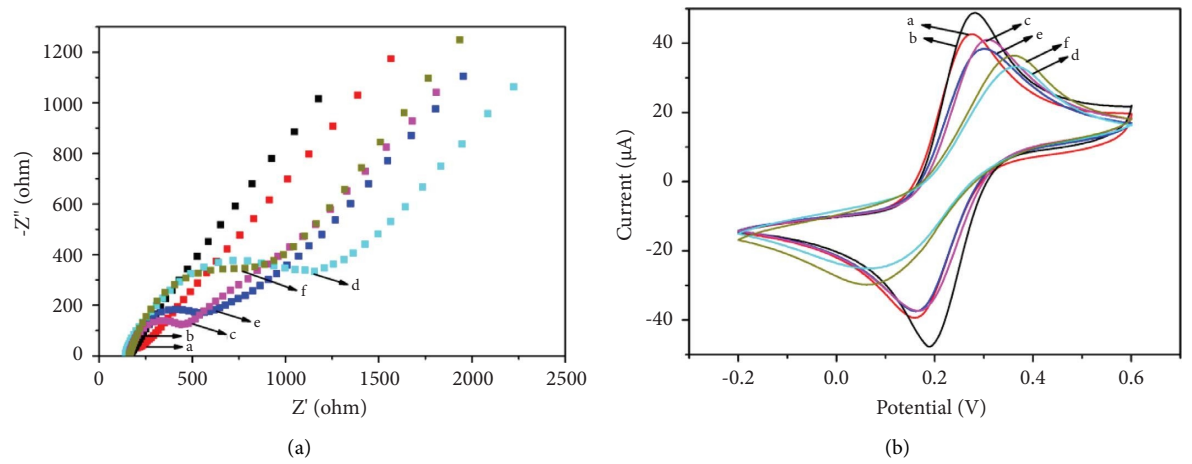

Figure 3: EIS (a) and CV (b) characteristics of different-modified electrode: (a) bare AuE, (b) AuNPs/AuE, (c) Fc-HP2/AuNPs/AuE, (d) MCH/Fc-HP2/AuNPs/AuE, (e) PSA-HP1-Exo III/MCH/Fc-HP2/AuNPs/AuE, and (f) MB-DNA/PSA-HP1-Exo III/MCH/Fc-HP2/AuNPs/AuE.

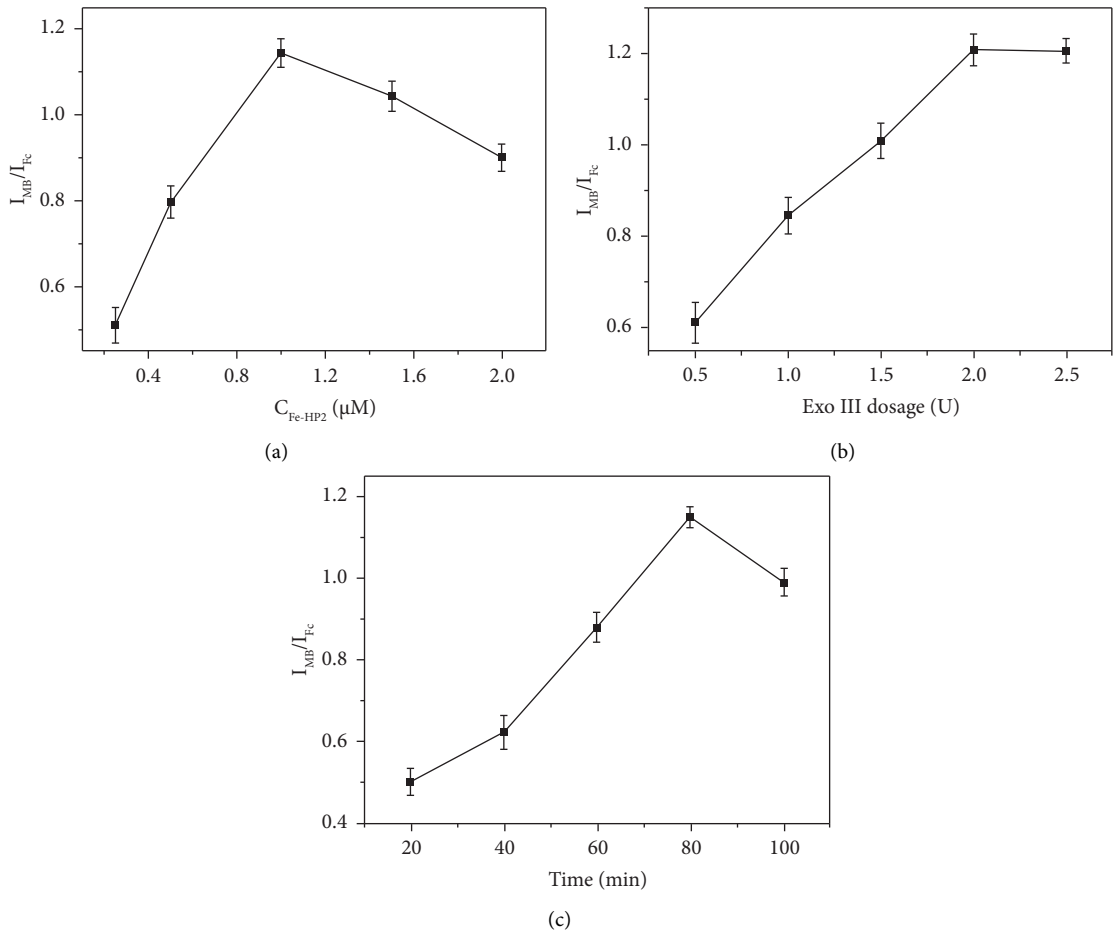

Figure 4: Optimization of the concentration of Fc-HP2 (a), the dosage of Exo III (b), and incubation time of Exo III (c).

reported PSA detection methods [35–41]. As shown in Table 1, the analytical performance of the aptasensor developed in this study was comparable or better than those of the reported methods.

3.6. Specificity, Reproducibility, and Stability Test. CEA, AFP, and HSA were employed as interferences to demonstrate the specificity of the proposed aptasensor. Although the concentration of the interferences (100 ng·mL−1) was 10-fold higher

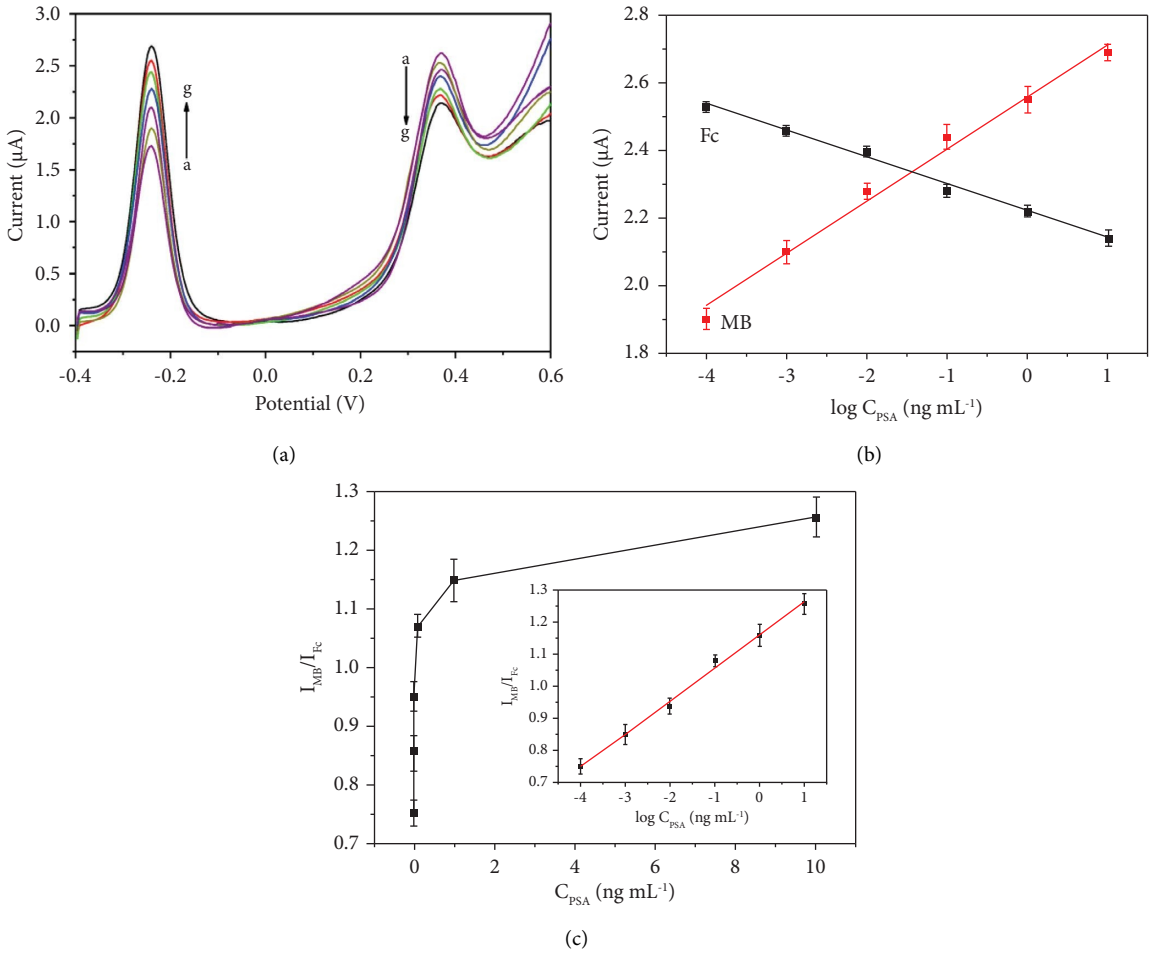

Figure 5: (a) SWV responses of the aptasensor to PSA standards with different concentrations ((a–g) 0, 100 fg·mL^{-1}, 1 pg·mL^{-1}, 10 pg·mL^{-1}, 100 pg·mL^{-1}, 1 ng·mL^{-1}, and 10 ng·mL^{-1}). (b) Relationship between the MB and Fc peak currents and the logarithm concentration of PSA. (c) The relation between I_{MB}/I_{Fc} and PSA concentrations (inset is the calibration plots between I_{MB}/I_{Fc} and the logarithm of PSA concentrations).

Table 1: Comparison of the analytical performances of PSA detection methods.

Analytical method	Linear range	LOD	References
PEC	0.01–50 ng·mL^{-1}	1.5 pg·mL^{-1}	[35]
PEC	0.001–10 ng·mL^{-1}	0.22 pg·mL^{-1}	[36]
ECL	0.005–1 ng·mL^{-1}	0.3 pg·mL^{-1}	[37]
ECL	0.005–50 ng·mL^{-1}	3.0 pg·mL^{-1}	[38]
ECL	0.01–10 pg·mL^{-1}	3.4 fg·mL^{-1}	[39]
Electrochemical	0.001–10 ng·mL^{-1}	0.67 pg·mL^{-1}	[40]
Electrochemical	0.001–10 ng·mL^{-1}	0.34 pg·mL^{-1}	[41]
Electrochemical	0.0001–10 ng·mL^{-1}	34.7 fg·mL^{-1}	This work

PEC: photoelectrochemical; ECL: electrochemiluminescence.

than that of PSA (10 ng·mL–1), their response signals were obviously lower than that of PSA (Figure 6), indicating acceptable specificity. The reproducibility of the aptasensor was investigated by using five aptasensors prepared under the same conditions to detect 1 ng·mL^{-1} PSA. The relative standard deviation (RSD) obtained was 3.3%, suggesting its good reproducibility. Furthermore, when the aptasensor was stored for 4°C for one and two weeks, it still maintained 90.5% and 85.1% of the original signal, respectively, indicating its good stability.

3.7. Analysis of Serum Samples. To assess the clinical application of the aptasensor in biological samples, three healthy human serum samples (obtained from Henan University of Science and Technology Hospital) were diluted 10-fold with 20 mM phosphate buffered saline (pH 7.4) and spiked with PSA. The recoveries were from 89.0% to 102.3% with a RSD of 2.1%–4.6% (Table 2), indicating the proposed aptasensor had good accuracy in clinical analysis.

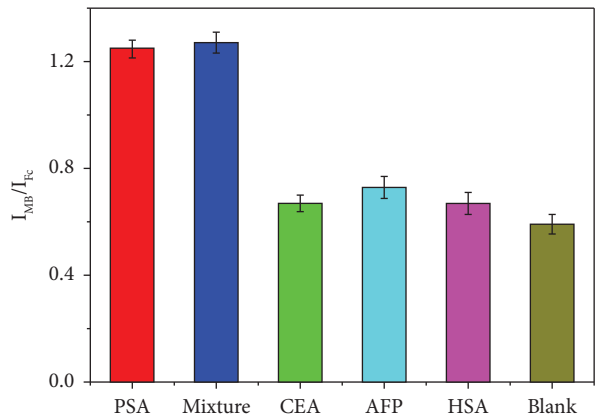

Figure 6: Specificity of the proposed aptasensor (PSA concentration was 10 ng·mL^{-1} and CEA, AFP, and HSA concentration was 100 ng·mL^{-1}, respectively).

Table 2: Electrochemical detection of PSA in human serum samples.

Sample	Added CEA	Detected CEA	Recovery (%)	RSD (%)
1	5.00 ng·mL^{-1}	4.91 ng·mL^{-1}	98.2	3.4
2	1.00 ng·mL^{-1}	0.89 ng·mL^{-1}	89.0	4.6
3	100.00 pg·mL^{-1}	102.30 pg·mL^{-1}	102.3	2.1

4. Conclusions

In summary, we constructed a simple ratiometric electrochemical aptasensor for ultrasensitive detection of PSA. Compared with conventional electrochemical aptasensors, this method only used two hairpin DNA probes and a MB-labeled DNA, thus reducing the measurement cost. Secondly, the ratiometric signal of I_{MB}/I_{Fc} was used to detect the target, which could improve the assay reproducibility and accuracy. Thirdly, the AuNPs-modified electrode provided a large surface area for Fc-HP2 immobilization and improved electron conductivity. The utilization of Exo III-assisted target recycling could further enhance the detection sensitivity. In addition, the proposed strategy had been applied to detect PSA in diluted human serum samples. Although good performances have been achieved, the present method required multiple hybridization and washing steps, which was the main limitation of the study. Further design of the simple and new aptamer-based assays for PSA detection might be the future scope.

Data Availability

The data used to support the findings of this study are available from the corresponding author upon request.

Conflicts of Interest

The authors declare that they have no conflicts of interest.

Authors' Contributions

Ping Wang was involved in methodology and investigation and wrote the original draft. Yaoyao Xie conducted experiments and assisted in the writing of the article. Zhimin Guan and Huikai Ma constructed figures and tables. Shoumin Xi conceptualized and supervised the study.

Acknowledgments

This work was supported by the National Natural Science Foundation of China (61701171).

References

[1] A. R. Jalalvand, F. Shokri, and A. Yari, "Co-operation of electrochemistry and chemometrics to develop a novel electrochemical aptasensor based on generation of first- and second-order data for selective and sensitive determination of the prostate specific antigen biomarker," *Microchemical Journal*, vol. 183, Article ID 108026, 2022.

[2] L. Yan, S. Xu, and F. Xi, "Disposal immunosensor for sensitive electrochemical detection of prostate-specific antigen based on amino-rich nanochannels array-modified patterned indium tin oxide electrode," *Nanomaterials*, vol. 12, no. 21, p. 3810, 2022.

[3] M. M. Webber, A. Waghray, and D. Bello, "Prostate-specific antigen, a serine protease, facilitates human prostate cancer cell invasion," *Clinical Cancer Research: An Official Journal of the American Association for Cancer Research*, vol. 1, no. 10, pp. 1089–1094, 1995.

[4] X. Tang, C. Lu, X. Xu et al., "A visible and near-infrared light dual responsive "signal-off" and "signal-on" photoelectrochemical aptasensor for prostate-specific antigen," *Biosensors and Bioelectronics*, vol. 202, Article ID 113905, 2022.

[5] L. F. Cheow, S. H. Ko, S. J. Kim, K. H. Kang, and J. Han, "Increasing the sensitivity of enzyme-linked immunosorbent assay using multiplexed electrokinetic concentrator," *Analytical Chemistry*, vol. 82, no. 8, pp. 3383–3388, 2010.

[6] D. S. Grubisha, R. J. Lipert, H. Y. Park, J. Driskell, and M. D. Porter, "Femtomolar detection of prostate-specific Antigen: an immunoassay based on surface-enhanced Raman scattering and immunogold labels," *Analytical Chemistry*, vol. 75, no. 21, pp. 5936–5943, 2003.

[7] N. Xia, D. Deng, Y. Wang, C. Fang, and S. J. Li, "Gold nanoparticle-based colorimetric method for the detection of prostate-specific antigen," *International Journal of Nanomedicine*, vol. 13, pp. 2521–2530, 2018.

[8] A. Liu, F. Zhao, Y. Zhao, L. Shangguan, and S. Liu, "A portable chemiluminescence imaging immunoassay for simultaneous detection of different isoforms of prostate specific antigen in serum," *Biosensors and Bioelectronics*, vol. 81, pp. 97–102, 2016.

[9] Q. Hu, S. Gan, Y. Bao, Y. Zhang, D. Han, and L. Niu, "Electrochemically controlled ATRP for cleavage-based electrochemical detection of the prostate-specific antigen at femtomolar level concentrations," *Analytical Chemistry*, vol. 92, no. 24, pp. 15982–15988, 2020.

[10] K. Chuah, L. M. Lai, I. Y. Goon, S. G. Parker, R. Amal, and J. Justin Gooding, "Ultrasensitive electrochemical detection of prostate-specific antigen (PSA) using gold-coated magnetic nanoparticles as 'dispersible electrodes'," *Chemical Communications*, vol. 48, no. 29, pp. 3503–3505, 2012.

[11] A. Moutsiopoulou, D. Broyles, E. Dikici, S. Daunert, and S. K. Deo, "Molecular aptamer beacons and their applications in sensing, imaging, and diagnostics," *Small*, vol. 15, no. 35, Article ID 1902248, 2019.

[12] W. Tan, M. J. Donovan, and J. Jiang, "Aptamers from cell-based selection for bioanalytical applications," *Chemical Reviews*, vol. 113, no. 4, pp. 2842–2862, 2013.

[13] Y. Wu, I. Belmonte, K. S. Sykes, Y. Xiao, and R. J. White, "Perspective on the future role of aptamers in analytical chemistry," *Analytical Chemistry*, vol. 91, no. 24, pp. 15335–15344, 2019.

[14] M. Pourmadadi, A. Nouralishahi, M. Shalbaf, J. Shabani Shayeh, and A. Nouralishahi, "An electrochemical aptasensor for detection of prostate-specific antigen-based on carbon quantum dots-gold nanoparticles," *Biotechnology and Applied Biochemistry*, vol. 70, no. 1, pp. 175–183, 2023.

[15] M. Majdinasab, M. Daneshi, and J. Louis Marty, "Recent developments in non-enzymatic (bio)sensors for detection of pesticide residues: focusing on antibody, aptamer and molecularly imprinted polymer," *Talanta*, vol. 232, Article ID 122397, 2021.

[16] R. M. Kong, L. Ding, Z. Wang, J. You, and F. Qu, "A novel aptamer-functionalized MoS2 nanosheet fluorescent biosensor for sensitive detection of prostate specific antigen," *Analytical and Bioanalytical Chemistry*, vol. 407, no. 2, pp. 369–377, 2015.

[17] A. Raouafi, A. Sánchez, N. Raouafi, and R. Villalonga, "Electrochemical aptamer-based bioplatform for ultrasensitive detection of prostate specific antigen," *Sensors and Actuators B: Chemical*, vol. 297, Article ID 126762, 2019.

[18] Y. Sun, J. Fan, L. Cui, W. Ke, F. Zheng, and Y. Zhao, "Fluorometric nanoprobes for simultaneous aptamer-based detection of carcinoembryonic antigen and prostate specific antigen," *Microchimica Acta*, vol. 186, pp. 1–10, 2019.

[19] M. Chen, Z. Tang, C. Ma, and Y. Yan, "A fluorometric aptamer based assay for prostate specific antigen based on enzyme-assisted target recycling," *Sensors and Actuators B: Chemical*, vol. 302, Article ID 127178, 2020.

[20] Z. Hong, G. Chen, S. Yu, R. Huang, and C. Fan, "A potentiometric aptasensor for carcinoembryonic antigen (CEA) on graphene oxide nanosheets using catalytic recycling of DNase I with signal amplification," *Analytical Methods*, vol. 10, no. 45, pp. 5364–5371, 2018.

[21] N. Wu, Y. T. Wang, X. Y. Wang, X. W. Chen, T. Yang, and J. H. Wang, "A simple, one-pot and ultrasensitive DNA sensor via Exo III-Assisted target recycling and 3D DNA walker cascade amplification," *Analytica Chimica Acta*, vol. 1147, pp. 15–22, 2021.

[22] Q. Pei, Y. Wang, S. Liu et al., "Exonuclease III-aided autonomous cascade signal amplification: a facile and universal DNA biosensing platform for ultrasensitive electrochemical detection of S. typhimurium," *New Journal of Chemistry*, vol. 41, no. 15, pp. 7613–7620, 2017.

[23] E. Xiong, X. Yan, X. Zhang, Y. Liu, J. Zhou, and J. Chen, "Exonuclease III–assisted cascade signal amplification strategy for label-free and ultrasensitive electrochemical detection of nucleic acids," *Biosensors and Bioelectronics*, vol. 87, pp. 732–736, 2017.

[24] R. Zhang, Y. Wang, X. Qu et al., "Exonuclease III-powered DNA walking machine for label-free and ultrasensitive electrochemical sensing of antibiotic," *Sensors and Actuators B: Chemical*, vol. 297, Article ID 126771, 2019.

[25] Q. Li, Z. Lu, X. Tan et al., "Ultrasensitive detection of aflatoxin B 1 by SERS aptasensor based on exonuclease-assisted recycling amplification," *Biosensors and Bioelectronics*, vol. 97, pp. 59–64, 2017.

[26] C. Liu, T. Wu, W. Zeng, J. Liu, B. Hu, and L. Wu, "Dual-signal electrochemical aptasensor involving hybridization chain reaction amplification for aflatoxin B1 detection," *Sensors and Actuators B: Chemical*, vol. 371, Article ID 132494, 2022.

[27] L. Wu, F. Ding, W. Yin et al., "From electrochemistry to electroluminescence: development and application in a ratiometric aptasensor for aflatoxin B1," *Analytical Chemistry*, vol. 89, no. 14, pp. 7578–7585, 2017.

[28] K. Shao, B. Wang, A. Nie et al., "Target-triggered signal-on ratiometric electrochemiluminescence sensing of PSA based on MOF/Au/G-quadruplex," *Biosensors and Bioelectronics*, vol. 118, pp. 160–166, 2018.

[29] K. Peng, P. Xie, Z. H. Yang, R. Yuan, and K. Zhang, "Highly sensitive electrochemical nuclear factor kappa B aptasensor based on target-induced dual-signal ratiometric and polymerase-assisted protein recycling amplification strategy," *Biosensors and Bioelectronics*, vol. 102, pp. 282–287, 2018.

[30] Y. Xu, Y. Zhang, N. Li et al., "An ultra-sensitive dual-signal ratiometric electrochemical aptasensor based on functionalized MOFs for detection of HER2," *Bioelectrochemistry*, vol. 148, Article ID 108272, 2022.

[31] C. Zhu, D. Liu, Y. Li et al., "Ratiometric electrochemical aptasensor for ultrasensitive detection of Ochratoxin A based on a dual signal amplification strategy: engineering the binding of methylene blue to DNA," *Biosensors and Bioelectronics*, vol. 150, Article ID 111814, 2020.

[32] X. Wang, Y. Li, M. Zhao et al., "An ultrafast ratiometric electrochemical biosensor based on potential-assisted hybridization for nucleic acids detection," *Analytica Chimica Acta*, vol. 1211, Article ID 339915, 2022.

[33] J. Zhang, D. Wang, and Y. Li, "Ratiometric electrochemical sensors associated with self-cleaning electrodes for simultaneous detection of adrenaline, serotonin, and tryptophan," *ACS Applied Materials and Interfaces*, vol. 11, no. 14, pp. 13557–13563, 2019.

[34] J. Zhang, S. Song, L. Wang, D. Pan, and C. Fan, "A gold nanoparticle-based chronocoulometric DNA sensor for amplified detection of DNA," *Nature Protocols*, vol. 2, no. 11, pp. 2888–2895, 2007.

[35] S. Lv, K. Zhang, Y. Zeng, and D. Tang, "Double photosystems-based 'Z-scheme' photoelectrochemical sensing mode for ultrasensitive detection of disease biomarker accompanying three-dimensional DNA walker," *Analytical Chemistry*, vol. 90, no. 11, pp. 7086–7093, 2018.

[36] B. Li, L. Guo, M. Chen, Y. Guo, L. Ge, and H. F. Kwok, "Single-atom Pt-anchored Zn0.5Cd0.5S boosted

photoelectrochemical immunoassay of prostate-specific antigen," *Biosensors and Bioelectronics*, vol. 202, Article ID 114006, 2022.

[37] L. Fu, X. Gao, S. Dong et al., "Coreactant-Free and direct electrochemiluminescence from dual-stabilizer-capped InP/ZnS nanocrystals: a new route involving n-type luminophore," *Analytical Chemistry*, vol. 94, no. 2, pp. 1350–1356, 2021.

[38] Y. Wang and X. Kan, "Sensitive and selective "signal-off" electrochemiluminescence sensing of prostate-specific antigen based on an aptamer and molecularly imprinted polymer," *Analyst*, vol. 146, no. 24, pp. 7693–7701, 2021.

[39] Z. Chang, C. Zhang, and B. Yao, "Novel dual-sensitization electrochemiluminescence immunosensor using photopermeable $Ru(bpy)_3^{2+}$-doped chitosan/SiO_2 nanoparticles as labels and chitosan-decorated Nafion/MWNTs composites as enhancer," *Luminescence*, vol. 37, no. 1, pp. 58–71, 2022.

[40] Y. Zheng, J. Wang, G. Chen et al., "DNA walker-amplified signal-on electrochemical aptasensors for prostate-specific antigen coupling with two hairpin DNA probe-based hybridization reaction," *Analyst*, vol. 147, no. 9, pp. 1923–1930, 2022.

[41] J. Feng, C. Chu, K. Dang, T. Yao, Z. Ma, and H. Han, "Responsive-released strategy based on lead ions-dependent DNAzyme functionalized UIO-66-NH2 for tumor marker," *Analytica Chimica Acta*, vol. 1187, Article ID 339170, 2021.